Friction stir processed Al - Metal oxide surface composites: Anodization and optical appearance

Gudla, Visweswara Chakravarthy; Jensen, Flemming; Canulescu, Stela; Simar, Aude; Ambat, Rajan

Published in:
Surface Modification Technologies XXVIII. Proceedings of the Twenty Eighth International Conference on Surface Modification Technologies

Publication date:
2014

Document Version
Peer reviewed version

Friction stir processed Al - Metal oxide surface composites: Anodization and optical appearance

Visweswara Chakravarthy Gudla[a], Flemming Jensen[a,b], Stela Canulescu[c], Aude Simar[d], Rajan Ambat[a*]

[a] Building 425, Produktionstorvet, Department of Mechanical Engineering, Technical University of Denmark, DK-2800 Kgs. Lyngby, Denmark

[b] Bang & Olufsen A/S, DK-7600, Struer, Denmark

[c] Department of Photonics Engineering, Technical University of Denmark, DK-4000 Roskilde, Denmark

[d] iMMC , Université Catholique de Louvain, 1348 Louvain-la-Neuve, Belgium

vichg@mek.dtu.dk, flj@bang-olufsen.dk, stec@fotonik.dtu.dk, aude.simar@uclouvain.be, *Corresponding author: ram@mek.dtu.dk (Tel: +45-45252181, Fax: +45-45936213)

Abstract

Multiple-pass friction stir processing (FSP) was employed to impregnate metal oxide (TiO_2, Y_2O_3 and CeO_2) particles into the surface of an Aluminium alloy. The surface composites were then anodized in a sulphuric acid electrolyte. The effect of anodizing parameters on the resulting optical appearance was studied. Microstructural and morphological characterization was performed using transmission electron microscopy (TEM). The surface appearance was analysed using an integrating sphere-spectrometer setup. Increasing the anodizing voltage changed the surface appearance of the composites from dark to greyish white. This is attributed to the localized microstructural and morphological differences around the metal oxide particles incorporated into the anodic alumina matrix. The metal oxide particles in the FSP zone electrochemically shadowed the underlying Al matrix and modified the local morphology of the anodic layer as well as changed the light interaction phenomenon.

Keywords

Aluminium, Friction Stir Processing, Spectrophotometry, Optical appearance, TiO_2, Y_2O_3, CeO_2, Reflectance, Electrochemical Finishing, Transmission Electron Microscopy, Composites, Decorative Anodizing, Sulphuric Acid, Focused Ion Beam

1.0. Introduction

Aluminium alloys are used in various applications due to their high mechanical strength to weight ratio. Surface finishing of Al by anodizing improves its corrosion and wear resistance and also adhesion to subsequent paint layers [1 2 3]. Sulphuric acid anodizing (SAA) provides a clear and transparent anodic oxide layer on the surface of Al which comprises a self-organized hexagonal porous structure (20-30 nm pore diameter) [4 5]. This porous structure is usually filled with dyes using capillary effect and later sealed in boiling water to impart colours to the anodized surface [6 7 8]. A wide range of colours, including black have been produced over the years but achieving a white glossy anodized Al surface is difficult. This is because white appearance is generated by scattering of light by particles that are bigger than the pores while colours are generated by selective absorption of particular wavelengths [9 10].

White anodized Al finds application in the aerospace and architectural industry where a low solar absorptance is preferred to prevent temperature rise and related thermal expansion of structural components [11] [12]. Also, it is of great interest for aesthetic purposes and decorative applications in the architectural industry for facades, window profiles etc. White anodized Al has been reported earlier using a mixture of electrolytes, but the reflectance from these surfaces is not very high [13] [14]. Alternate processes based on Plasma Electrolytic Oxidation (PEO) and Micro Arc Oxidation (MAO), which are commercially available reported grey to white anodized surfaces. However the surfaces generated by these methods are not glossy and have a very high surface roughness [15] [16] [17] [18].

The glossy white anodized surface requires scattering of incident light within the anodic layer and also generate a surface gloss due to specular reflectance from a smooth surface without any absorption in the visible wavelength region [19] [20] [21]. One approach for achieving this is to mimic the optical scattering phenomenon from white paints which contain a pigment in a polymer matrix. The pigments used should have a high refractive index difference with the surrounding polymer matrix and enable very efficient scattering. Similar scattering effects can be achieved using high refractive index metal oxides (based on Ti, Y and Ce) in anodic alumina which has a refractive index similar to polymer matrix of paints [22] [23] [24]. To obtain such a structure on the anodized Al surface, metal oxide particles need to be incorporated into the Al matrix prior to anodizing and the obtained composite be later anodized to reveal these particles in a transparent anodic alumina matrix (similar to paints).

Incorporation of metal oxides powders into metal matrices has been of interest to many researchers due to the enhanced mechanical properties of the obtained composites by particle reinforcement. Various techniques have been employed to prepare many composite systems [25] [26] [27] [28] [29] [30]. Friction stir processing (FSP) is one such technique that has been extensively used for preparation of composites [31] [32] [33] [34] [35]. FSP allows for semi solid state mixing of the involved phases and the maximum temperature involved for Al based composites processing is up to 450 °C -500 °C[36]. However, use of this technique to obtain composite surfaces for white anodizing of Al has not yet been attempted.

In the current work we present the initial findings on use of metal oxides incorporation into anodic alumina for white anodized surface finish. The effect of anodizing parameters on the obtained optical appearance is studied. Transmission electron microscopy (TEM) was used to investigate the structure and morphology of the anodized composites. Surface appearance was characterized using reflectance spectroscopy and the obtained surface appearance is explained in terms of morphological features of the anodic layer.

2.0. Experimental

2.1. Materials

Aluminium substrates (Peraluman™ 853, Alcan rolled products, Germany) with dimensions 200 mm x 60 mm x 6 mm were obtained in rolled condition. Commercial metal oxide powders TiO_2 (300 nm, Ti-pure R796, DuPont Titanium Technologies, Belgium), Y_2O_3 (0.5-1 µm, SkySpring Nanomaterials, Inc., USA) and CeO_2 (200-300 nm, Nano-Oxides, Inc, USA) were used. Particle size distributions were chosen based on the refractive index and their related light scattering power.

2.2. Friction Stir Processing

FSP was performed using a Hermle milling machine equipped with a steel tool having 20 mm shoulder diameter, 1.5 mm pin length with a M6 thread and three flats. The backwards tilt angle of the tool was maintained at 1˚. A groove 0.5 mm deep, 10 mm wide and 180 mm long in the substrates was filled with the powders (see Figure 1). The filled substrates were then covered by the same Al sheet rolled down to a thickness of 0.25 mm to prevent loss of powders during the initial FSP pass. Rotational speed of the tool was 1000 rpm and the advancing speed was 200 mm/min for the first pass and 1000 mm/min for the next six passes. A surface of 175 mm long x 20 mm wide was processed for each pass with a total processing time of roughly 2 min. All seven passes were performed one over the other without any shift.

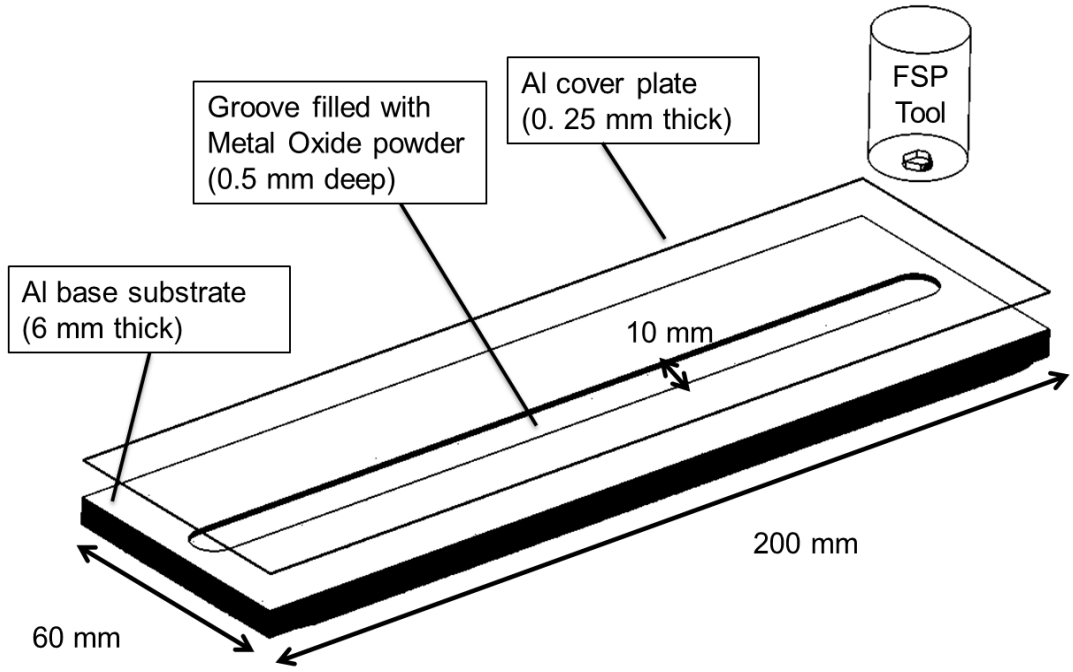

Figure 1: Schematic showing the setup with sample substrate and groove used for friction stir processing of Al- Metal Oxide surface composites.

2.3. Anodizing

The processed composite surfaces were polished and buffed to a mirror finish and subsequently degreased in a mild Alficlean™ solution at 60 ˚C. Desmutting was performed by immersing in dilute HNO_3 followed by demineralised water rinsing. Anodizing was carried out in a 20 wt.% sulphuric acid bath maintained at 18 ˚C. Three different anodizing voltages of 10 V, 15 V, and 19 V were used to obtain approx. 5 µm of anodized layer. After anodizing, the samples were rinsed with demineralized water. Sealing of the anodized layer was performed in water at 96 ˚C for 25 min followed by drying with hot air.

2.4. Reflectance Spectroscopy

Optical appearance of the processed composites after anodizing was analysed using an integrating sphere-spectrometer setup. The samples were illuminated at 8˚ incidence, with light from a Deuterium-Tungsten halogen light source (DH 2000, Ocean optics). Reflected light from the samples was collected and analysed for diffuse and total reflectance using a spectrometer (QE 65000, Ocean Optics). The wavelength range analysed was 350-750 nm

and was integrated over a period of 4 s. The spectrophotometer was calibrated using NIST standards.

2.5. Transmission Electron Microscopy

Transmission electron microscopy was carried out on the sample cross section in the anodized as well as non-anodized regions using a TEM (Model Tecnai G2 20) operating at 200 keV. The lamella for TEM were prepared using FIB-SEM in situ lift out (Model Quanta 200 3D DualBeam, FEI) and further thinned for electron transparency in a FIB-SEM (Helios Nanolab DualBeam, FEI).

3.0. Results

3.1. Visual Appearance

The visual appearance of the FSP samples after anodizing is shown in Figure 2. The FSP zone shows a different appearance for all three powders when compared to the adjacent unprocessed Al. The processed zone can be clearly identified (region between dotted lines) as it shows macroscopic semi-circular striations. For all the three powders types used, the anodized appearance shifts from dark to greyish white as the anodizing voltage is increased from 10 V to 19 V. This effect is most prominent in the case of surface containing TiO_2 powders where there is a clear difference between the surfaces anodized at 10 V and 15 V.

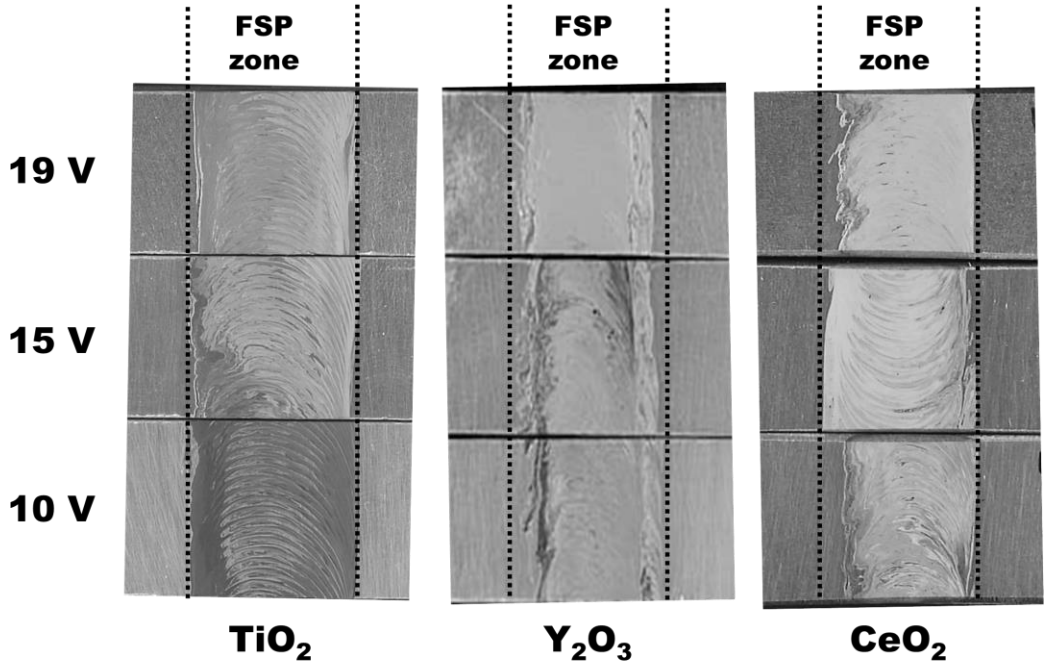

Figure 2: Visual appearance of the friction stir processed samples with different powders after sulphuric acid anodizing at different voltages.

3.2. Reflectance Spectroscopy

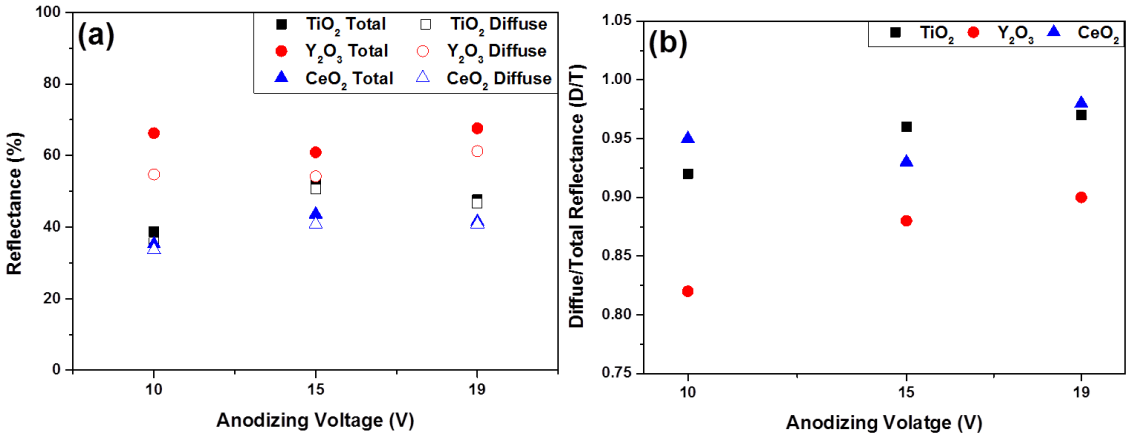

Figure 3: (a) Total and diffuse reflectance values (wavelength ~ 555 nm) and (b) Diffuse to Total reflectance (D/T) ratio obtained from the FSP surfaces after sulphuric acid anodizing at different voltages.

The reflectance values (at 555 nm) obtained from the spectrophotometry data are presented in Figure 3 (a). It can be seen that the total reflectance of the anodized surface increases from anodizing at 10 V to 15 V and then slightly reduces at 19 V for TiO_2 and CeO_2. However, for samples containing Y_2O_3, the total reflectance is lower at 15 V anodizing when compared to the 10 V and 19 V anodizing. The diffuse to total reflectance ratio which is a measure of how well the surface scatters light is shown in Figure 3 (b). It can be observed that the diffuse reflectance component for the Y_2O_3 containing surfaces is lower than that for TiO_2 and CeO_2 even though their total reflectance value is lower.

3.3. Transmission Electron Microscopy

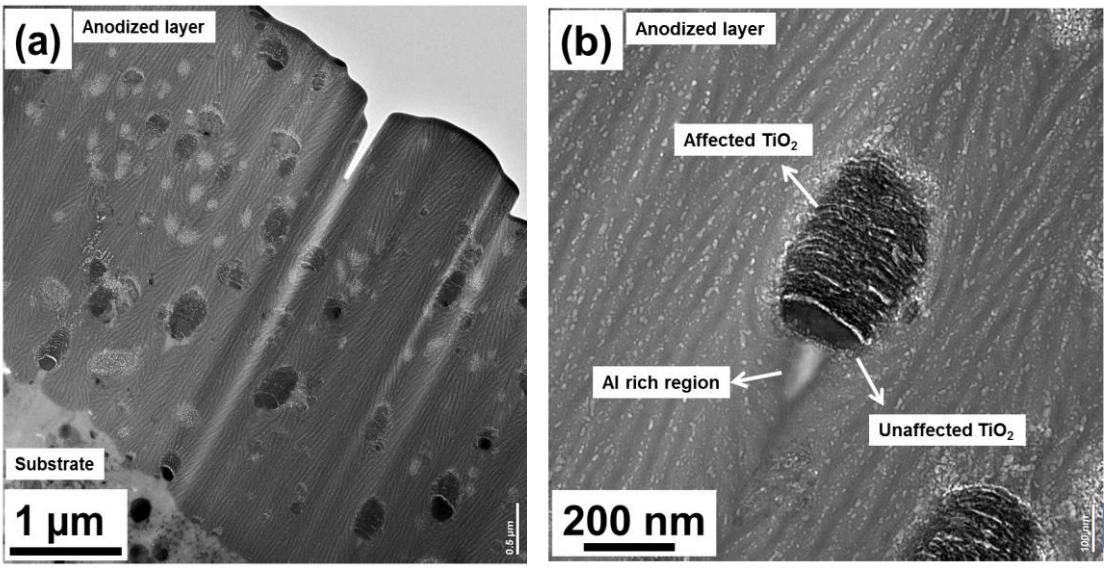

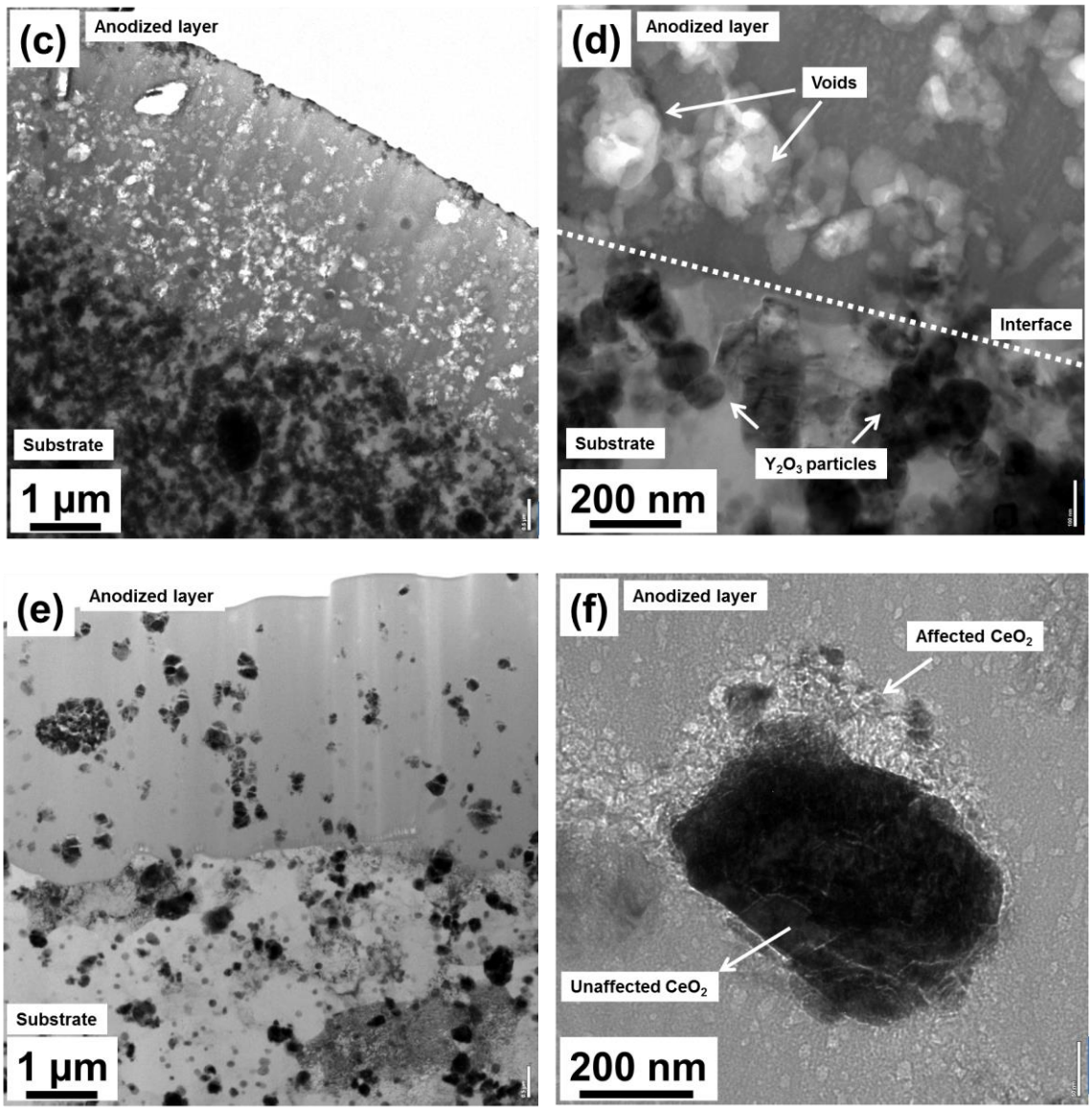

Figure 4: TEM bright field image showing anodized layer cross section of FSP and anodized samples with (a), (b) TiO_2, 19 V, (c), (d) Y_2O_3, 10 V and (e), (f) CeO_2 10 V.

The anodized layer on FSP surface containing TiO_2 and anodized at 19 V (Figure 4 (a)) shows different morphological features for the TiO_2 particles. In this case, the particles present in the anodized layer are fully or partially transformed. Typical features of the TiO_2 particle in Figure 4 (b) show that the particle is partially affected (top region of the particle) by the anodizing process. Also, the picture shows a bright region below the TiO_2 particle. Elemental analysis of the bright regions using energy dispersive spectroscopy (EDS) technique, show presence of very high content of Al compared to surrounding regions which showed Al, Ti and O.

The anodized layer on the sample containing Y_2O_3 particles is shown in Figure 4 (c). Unlike the TiO_2 containing sample, the Y_2O_3 particles are not present in the anodized layer. The anodized layer shows large number of voids, although the FSP substrate shows good distribution of Y_2O_3 particles (Figure 4 (d)). The voids are expected to be the result of expulsed Y_2O_3 particles during the anodizing process. For the samples containing CeO_2, anodizing at 10 V showed similar morphological features as for the TiO_2 particles (Figure 4

(e)). One of the CeO_2 particles shown in Figure 4 (f) appears affected (top region of the particle) by the anodizing process. However, regions of high Al content like those observed beneath the TiO_2 particles have not been observed in the anodized layer of CeO_2 containing samples.

4.0. Discussion

Friction stir processing (FSP) of Al substrate with metal oxide powders resulted in a surface composite with good distribution of particles in the processed zone. Anodizing of these composite surfaces visually revealed macroscopic inhomogeneity in the processed zone in terms of semi-circular striations (Figure 2). The striations are caused by the forward movement of the tool that generates a trail behind it. Overall distribution of particles in the FSP zone is uniform without any significant agglomeration (Figure 4). In all the cases, upon visual observation the surface appearance changed from dark to greyish white with increasing anodizing voltage. Reflectance spectroscopy data (Figure 3) measured by the integrating sphere setup showed that the reflectance values are highest for the Y_2O_3 containing surfaces when compared to the TiO_2 and CeO_2 containing surfaces irrespective of the anodizing voltage used. For anodized surfaces containing TiO_2 and CeO_2 the reflectance increased from 10 V to 15 V anodizing and later decreased from 15 V to 19 V anodizing. However for the Y_2O_3 containing samples, the reflectance was lowest for anodizing at 15 V. The TEM images shown in Figure 4 reveal that the morphology of the anodic layer and particles is different for different powders used. For Y_2O_3 powders the anodized layer showed very little presence of the particles. Surfaces containing TiO_2 and CeO_2 showed partially affected particles in the anodic layer. Also, un-anodized Al rich regions were observed beneath the TiO_2 particles in the anodized layer.

The difference in reflectance values measured from the anodized surfaces containing different powders is a manifestation of various factors like the refractive index of the powders, the distribution and concentration of the powders, the roughness of the surface and the interface between anodized layer and substrate, morphology of the anodized layer as well as of the powder particles [9] [10]. High refractive index particles in a visibly transparent medium scatter light and increase the diffuse reflectance. The increased scattering is due to the refractive index difference between the particle and the surrounding medium. In the present case, the metal oxide particles have a higher refractive index when compared to anodic alumina (η=1.6-1.7) [37] [38] and hence result in a high diffuse reflectance value. However, the total reflectance value measured is only 40-60% of the incident light intensity. The loss of intensity can be explained by the morphological features observed in the anodic layer. In the case of anodized layer with TiO_2, regions of high Al content observed beneath the particles act as absorption centres for light. Anodic alumina is a transparent medium under visible light, but Al as a metal has a very high optical extinction coefficient. This coupled with the sub-micron size of the metallic Al region leads to an effective extinction of light and hence the reduced loss of reflected intensity [39] [40] [41] [42] [43]. The presence of these metallic Al regions in anodic alumina depends on the anodizing voltage as the oxidation power of the process increases with anodizing voltage [44] [45]. At lower anodizing voltages the oxidative power is not sufficient to fully anodize the Al beneath the insulating TiO_2 particles owing to the current field distribution [46]. Hence, an increased amount of such metallic Al in anodized layer results in higher absorption of light and thus the reduced reflectance values. As the anodizing voltage increases, it is assumed that the Al surrounding the TiO_2 particle gets completely anodized increasing the reflectance. The Y_2O_3 containing anodized surfaces show no such Al rich regions and also have a higher reflectance values. This is due to the absence of any insulating particles in the anodized layer as seen in Figure 4 (c). Also, as the particles have

been removed from the matrix during the anodizing process, the diffuse reflectance obtained in this case is due to the scattering from voids rather than the particles themselves. A lower diffuse reflectance component observed for the Y_2O_3 containing surfaces (Figure 3 (b)) is due to the fact that the incident light is now reflected from the anodized layer – metal substrate interface, which is similar to the reflection from a smooth metal surface which appears glossy (specular). The phenomenon of transformation of crystalline TiO_2 and CeO_2 particles to amorphous phase and also the removal of Y_2O_3 particles after anodizing of these composites is yet to be understood and requires more detailed analysis. One possible explanation for the visible transformation of TiO_2 to amorphous phase is that it is known to be soluble in sulphuric acid, and the combined effect of the acid with the external applied anodizing voltage can cause dissolution and re-precipitation in amorphous phase of the oxide. For the Y_2O_3 particles it was observed that their morphology is very porous and this can be the reason for their leaching out into the electrolyte from the matrix due to the acid and voltage applied.

Refractive index of TiO_2 (η=2.6-2.9) [47] is higher than that of CeO_2 (η=2.2-2.4) [48] and hence the scattering efficiency of the anodized Al-TiO_2 system would be better than that of anodized Al-CeO_2 system. However, from the reflectance values, only slight difference was observed at a given voltage. This could be attributed to the transformation of TiO_2 to amorphous phase in the anodic alumina with a reduced refractive index (η=2.42) [49 50].

A white glossy anodized Al surface would have a total reflectance of 80-90% with a very high diffuse reflectance component. The values obtained for such surfaces using metal oxide incorporation into Al matrix before anodizing have been shown to be max. 50%. Use of Y_2O_3 gives higher reflectance value, but the voids generated reduce the mechanical properties of the anodic alumina layer. When comparing between TiO_2 and CeO_2, it has been observed that the reflectance values do not differ considerably. However high values of reflectance would be achieved if higher particle concentrations are used and the crystalline nature of the oxide particles is retained after anodizing.

5.0. Conclusions

- Friction stir processing was employed to prepare Al with Ti, Y and Ce oxide surface composites with little or no agglomerations of particles.
- Sulphuric acid anodizing of the prepared surface composites showed an increase in surface brightness with increasing anodizing voltage.
- High resolution TEM analysis show that the anodizing process transformed the TiO_2 and CeO_2 particles to an amorphous state, while the Y_2O_3 particles were removed from the Al matrix during anodizing.
- Anodizing at lower voltages showed the presence of un-anodized crystalline Al regions below the TiO_2 particles.
- Presence of metallic Al in the anodic alumina along with the reduced refractive index of TiO_2 and CeO_2 particles resulted in reduced reflectance of anodized surface.
- The Y_2O_3 containing surfaces showed higher reflectance due to scattering from the voids in the anodic layer and reflection from the anodic layer-metal substrate interface.

Acknowledgements

The authors would like to thank the Danish National Advanced Technology Foundation for their financial support in the ODAAS project and all the involved project

partners. Dr. Jørgen Schou is acknowledged for help with reflectance spectroscopy measurements. Prof. Aude Simar acknowledges the financial support from the Interuniversity Attraction Poles Program from the Belgian State through the Belgian Policy agency; contract IAP7/21 “INTEMATE”.

References

(1) Wernick, S.; Pinner, R.; Sheasby, P. G.; International., A. S. M. *The surface treatment and finishing of aluminium and its alloys 1-2*; Finishing Publ: Teddington, 1987; pp. 1–47+1273 s. – I 2 bd.
(2) Mohagheghi, S.; Hatefi, A.; Kianvash, A. Effect of H_3PO_4 anodising variations on Al-epoxy adhesion strength Surf. Eng. **2013**, *29*, 737–742.
(3) Spies, H.-J. Surface engineering of aluminium and titanium alloys: an overview Surf. Eng. **2010**, *26*, 126–134.
(4) Grubbs, C. A. Anodizing of aluminum Met. Finish. **2007**, *105*, 397–412.
(5) Canulescu, S.; Rechendorff, K.; Borca, C. N.; Jones, N. C.; Bordo, K.; Schou, J.; Pleth Nielsen, L.; Hoffmann, S. V.; Ambat, R. Band gap structure modification of amorphous anodic Al oxide film by Ti-alloying Appl. Phys. Lett. **2014**, *104*, 121910.
(6) Thompson, G.; Wood, G. Porous anodic film formation on aluminium Nature **1981**, *290*.
(7) Selvam, M. Colouring of anodised aluminium by electroless method Surf. Eng. **2011**, *27*, 711–718.
(8) Rezagholi, H.; Zangeneh-Madar, K.; Mirjani, M.; Ahangarkani, M. Study on electropolished/anodised aluminium foil before and after dyeing Surf. Eng. **2014**, *30*.
(9) Hecht, E. *Optics*; Addison Wesley, 2002.
(10) Tilley, R. *Colour and the Optical Properties of Materials. An exploration of relationship between light, the optical properties of material and colour. Cardiff University*; 1999.
(11) Kaysser, W. Surface modifications in aerospace applications Surf. Eng. **2001**, *17*, 305–312.
(12) Sharma, A. K. Surface engineering for thermal control of spacecraft Surf. Eng. **2005**, *21*, 249–253.
(13) Siva Kumar, C.; Mayanna, S. M.; Mahendra, K. N.; Sharma, A. K.; Uma Rani, R. Studies on white anodizing on aluminum alloy for space applications Appl. Surf. Sci. **1999**, *151*, 280–286.
(14) Siva Kumar, C.; Sharma, A. K.; Mahendra, K. N.; Mayanna, S. M. Studies on anodic oxide coating with low absorptance and high emittance on aluminum alloy 2024 Sol. Energy Mater. Sol. Cells **2000**, *60*, 51–57.
(15) Yerokhin, A. L.; Nie, X.; Leyland, A.; Matthews, A.; Dowey, S. J. Plasma electrolysis for surface engineering Surf. Coatings Technol. **1999**, *122*, 73–93.
(16) Wheeler, J. M.; Curran, J. a.; Shrestha, S. Microstructure and multi-scale mechanical behavior of hard anodized and plasma electrolytic oxidation (PEO) coatings on aluminum alloy 5052 Surf. Coatings Technol. **2012**, *207*, 480–488.
(17) Malayoglu, U.; Tekin, K. C.; Malayoglu, U.; Shrestha, S. An investigation into the mechanical and tribological properties of plasma electrolytic oxidation and hard-anodized coatings on 6082 aluminum alloy Mater. Sci. Eng. A **2011**, *528*, 7451–7460.
(18) Kharanagh, V. J.; Sani, M. A. F.; Rafizadeh, E. Effect of current frequency on coating properties formed on aluminised steel by plasma electrolytic oxidation Surf. Eng. **2013**, *30*, 224–228.
(19) Muller, K.; Silvennoinen, R.; Peiponen, K. E. *Specular Gloss*; 2008.

(20) *Specular Gloss - Light Reflection From an Ideal Surface*; Silvennoinen, R.; Peiponen, K.; Muller, K., Eds.; Elsevier: Amsterdam, 2008; pp. 5–51.
(21) *Specular Gloss - Light Reflection From a Rough Surface*; Silvennoinen, R.; Peiponen, K.; Muller, K., Eds.; Elsevier: Amsterdam, 2008; pp. 53–77.
(22) Diebold, U. The surface science of titanium dioxide Surf. Sci. Rep. **2003**, *48*, 53–229.
(23) Winkler, J. *Titanium dioxide*; Vincentz Verlag, Hannover, 2003.
(24) Yao, J. K.; Huang, H. L.; Ma, J. Y.; Jin, Y. X.; Zhao, Y. A.; Shao, J. D.; He, H. B.; Yi, K.; Fan, Z. X.; Zhang, F.; Wu, Z. Y. High refractive index TiO_2 film deposited by electron beam evaporation Surf. Eng. **2009**, *25*, 257–260.
(25) Reddy, B. S. B.; Das, K.; Das, S. A review on the synthesis of in situ aluminum based composites by thermal, mechanical and mechanical–thermal activation of chemical reactions J. Mater. Sci. **2007**, *42*, 9366–9378.
(26) Maity, P. C.; Panigrahi, S. C.; Chakraborty, P. N. Preparation of aluminium-alumina in-situ particle composite by addition of titania to aluminium melt Scr. Metall. Mater. **1993**, *28*, 549–552.
(27) Maity, P. C.; Chakraborty, P. N.; Panigrahi, S. C. Processing and properties of Al-Al_2O_3 (TiO_2) in situ particle composite J. Mater. Process. Technol. **1995**, *53*, 857–870.
(28) Feng; Froyen. Formation of Al_3Ti and Al_2O_3 from an Al-TiO_2 system for preparing in-situ aluminium matrix composites Compos. Part A (Applied Sci. Manuf. **2000**, *31A*, 385–390.
(29) Ying, D.; Zhang, D.; Newby, M. Solid-state reactions during heating mechanically milled Al/TiO2 composite powders Metall. Mater. Trans. … **2004**, *35*, 2115–2125.
(30) Chen, C. F.; Kao, P. W.; Chang, L. W.; Ho, N. J. Effect of Processing Parameters on Microstructure and Mechanical Properties of an Al-$Al_{11}Ce_3$-Al_2O_3 In-Situ Composite Produced by Friction Stir Processing Metall. Mater. Trans. A **2010**, *41*, 513–522.
(31) Arora, H. S.; Singh, H.; Dhindaw, B. K. Composite fabrication using friction stir processing—a review Int. J. Adv. Manuf. Technol. **2011**, *61*, 1043–1055.
(32) Ma, Z. Y. Friction Stir Processing Technology: A Review Metall. Mater. Trans. A **2008**, *39*, 642–658.
(33) Mishra, R.; Ma, Z.; Charit, I. Friction stir processing: a novel technique for fabrication of surface composite Mater. Sci. Eng. A **2003**, *341*, 307–310.
(34) Lee, I. S.; Kao, P. W.; Ho, N. J. Microstructure and mechanical properties of Al–Fe in situ nanocomposite produced by friction stir processing Intermetallics **2008**, *16*, 1104–1108.
(35) Hsu, C. J.; Chang, C. Y.; Kao, P. W.; Ho, N. J.; Chang, C. P. Al–Al_3Ti nanocomposites produced in situ by friction stir processing Acta Mater. **2006**, *54*, 5241–5249.
(36) Mishra, R. S.; Ma, Z. Y. Friction stir welding and processing Mater. Sci. Eng. R Reports **2005**, *50*, 1–78.
(37) Pastore, G. F. Transmission interference spectrometric determination of the thickness and refractive index of barrier films formed anodically on aluminum Thin Solid Films **1985**, *123*, 9–17.
(38) Khan, I. H.; Leach, J. S. L.; Wilkins, N. J. M. The thickness and optical properties of films of anodic aluminium oxide Corros. Sci. **1966**, *6*, 483–497.
(39) Chang, R.; Hall, W. F. On the correlation between optical properties and the chemical/metallurgical constitution of multi-phase thin films Thin Solid Films **1977**, *46*, L5–L8.
(40) Saito, M.; Shiga, Y.; Miyagi, M. Unoxidized Aluminum Particles in Anodic Alumina Films J. Electrochem. Soc. **1993**, *140*, 1907–1911.

(41) Gudla, V. C.; Canulescu, S.; Shabadi, R.; Rechendorff, K.; Schou, J.; Ambat, R. Anodization and Optical Appearance of Sputter Deposited Al-Zr Coatings Light Met. **2014**, 369–373.
(42) Aggerbeck, M.; Junker-Holst, A.; Nielsen, D. V.; Gudla, V. C.; Ambat, R. Anodisation of sputter deposited aluminium–titanium coatings: Effect of microstructure on optical characteristics Surf. Coatings Technol. **2014**, *254*, 138–144.
(43) Gudla, V. C.; Canulescu, S.; Shabadi, R.; Rechendorff, K.; Dirscherl, K.; Ambat, R. Structure of anodized Al-Zr sputter deposited coatings and effect on optical appearance Appl. Surf. Sci. **2014,** In press.
(44) Walmsley, J. C.; Simensen, C. J.; Bjørgum, a.; Lapique, F.; Redford, K. The Structure and Impurities of Hard DC Anodic Layers on AA6060 Aluminium Alloy J. Adhes. **2008**, *84*, 543–561.
(45) Shimizu, K.; Brown, G. M.; Kobayashi, K.; Skeldon, P.; Thompson, G. E.; Wood, G. C. Ultramicrotomy—a route towards the enhanced understanding of the corrosion and filming behaviour of aluminium and its alloys Corros. Sci. **1998**, *40*, 1049–1072.
(46) Regonini, D.; Adamaki, V.; Bowen, C. R.; Pennock, S. R.; Taylor, J.; Dent, A. C. E. AC electrical properties of TiO_2 and Magnéli phases, Ti_nO_{2n-1} Solid State Ionics **2012**, *229*, 38–44.
(47) Palik, E. D. Chapter 2 - Refractive Index, Handbook of Optical Constanst of Solids, 1997, 5–114.
(48) Hass, G.; Ramsey, J. B.; Thun, R. Optical Properties and Structure of Cerium Dioxide Films J. Opt. Soc. Am. **1958**, *48*, 324–326.
(49) Bradley, J. D. B.; Evans, C. C.; Choy, J. T.; Reshef, O.; Deotare, P. B.; Parsy, F.; Phillips, K. C.; Loncar, M.; Mazur, E. Submicrometer-wide amorphous and polycrystalline anatase TiO_2 waveguides for microphotonic devices Opt. Express **2012**, *20*, 23821–23831.
(50) Fitzgibbons, E. T.; Sladek, K. J.; Hartwig, W. H. TiO_2 Film Properties as a Function of Processing Temperature J. Electrochem. Soc. **1972**, *119*, 735–739.